Molecular and Cellular Biology

The Spt5 C-Terminal Region Recruits Yeast 3′ RNA Cleavage Factor I

Andreas Mayer, Amelie Schreieck, Michael Lidschreiber, Kristin Leike, Dietmar E. Martin and Patrick Cramer

Mol. Cell. Biol. **2012, 32(7):1321. DOI: 10.1128/MCB.06310-11.**
Published Ahead of Print 30 January 2012.

MCB
Journals.ASM.org

The Spt5 C-Terminal Region Recruits Yeast 3′ RNA Cleavage Factor I

Andreas Mayer, Amelie Schreieck, Michael Lidschreiber, Kristin Leike, Dietmar E. Martin, and Patrick Cramer

Gene Center and Department of Biochemistry, Center for Integrated Protein Science Munich, Ludwig-Maximilians-Universität München, Munich, Germany

During transcription elongation, RNA polymerase II (Pol II) binds the general elongation factor Spt5. Spt5 contains a repetitive C-terminal region (CTR) that is required for cotranscriptional recruitment of the Paf1 complex (D. L. Lindstrom et al., Mol. Cell. Biol. 23:1368–1378, 2003; Z. Zhang, J. Fu, and D. S. Gilmour, Genes Dev. 19:1572–1580, 2005). Here we report a new role of the Spt5 CTR in the recruitment of 3′ RNA-processing factors. Chromatin immunoprecipitation (ChIP) revealed that the Spt5 CTR is required for normal recruitment of pre-mRNA cleavage factor I (CFI) to the 3′ ends of *Saccharomyces cerevisiae* genes. RNA contributes to CFI recruitment, as RNase treatment prior to ChIP further decreases CFI ChIP signals. Genome-wide ChIP profiling detected occupancy peaks of CFI subunits around 100 nucleotides downstream of the polyadenylation (pA) sites of genes. CFI recruitment to this defined region may result from simultaneous binding to the Spt5 CTR, to nascent RNA containing the pA sequence, and to the elongating Pol II isoform that is phosphorylated at serine 2 (S2) residues in its C-terminal domain (CTD). Consistent with this model, the CTR interacts with CFI *in vitro* but is not required for pA site recognition and transcription termination *in vivo*.

During transcription of protein-coding genes, RNA polymerase II (Pol II) associates with many factors, including elongation factors, RNA-processing factors, and chromatin-modifying enzymes (42, 66, 80). Many of these factors are recruited by binding to the C-terminal repeat domain (CTD), a tail-like extension of the largest Pol II subunit that is highly phosphorylated during elongation (10, 18, 54). Some elongation factors, including TFIIS (34) and Spt5 (36, 51), also bind the body of Pol II.

The gene encoding Spt5 was identified in *Saccharomyces cerevisiae* as a suppressor of transposon insertion in the promoter region of the *HIS4* gene (86). Spt5 is an essential nuclear protein (77) and binds Spt4 (24). Spt5 associates with Pol II *in vivo*, and mutations lead to a slow-growth phenotype in the presence of the nucleotide-depleting drug 6-azauracil (6-AU), arguing for a role for Spt5 in transcription elongation (24). The human homolog of yeast Spt4/5 affects Pol II elongation (83). Chromatin immunoprecipitation (ChIP) revealed that Spt5 colocalizes with Pol II throughout the transcribed region and past the polyadenylation (pA) site (35, 52, 68, 81). Spt4/5 is present on all transcribed yeast genes and is a general component of the elongation complex (52, 81). Spt4/5 also associates with Pol I (82) and Pol I genes (74).

Spt5 is the only known Pol II-associated factor that is conserved in all three kingdoms of life (85). The bacterial Spt5 homolog NusG and archaeal Spt5 consist of an N-terminal (NGN) domain and a flexibly linked C-terminal Kyrpides-Ouzounis-Woese (KOW) domain (38, 59). The structures of archaeal Spt4/5 bound to RNA polymerase or its clamp domain are known (36, 51). These structures indicate that the NGN domain closes the active center cleft to lock nucleic acids and render the elongation complex stable and processive (26, 36, 51). Eukaryotic Spt5 possesses additional regions and domains. Yeast Spt5 consists of an acidic N-terminal region, followed by an NGN domain, five KOW domains, and a repetitive C-terminal region (CTR) (69, 77, 89).

Spt5 has recently emerged as a platform that recruits factors to elongating Pol II. Spt5 copurifies with over 90 yeast proteins that are involved in transcription elongation, RNA processing, transcription termination, and mRNA export (44). Spt4/5 interacts with the histone chaperone Spt6 to modulate chromatin structure (24, 78). Spt5 colocalizes with Spt6 and Pol II at transcriptionally active loci on *Drosophila melanogaster* polytene chromosomes (5, 31). Spt5 interacts with the capping enzyme (65, 84) and recruits the Paf1 complex (45, 89). Mammalian Spt5 recruits the activation-induced cytidine deaminase to DNA during antibody gene diversification (64). Yeast Spt4/5 recruits She2 to nascent RNA, coupling mRNA localization with Pol II transcription (76).

Recruitment of factors can be mediated by the CTR of Spt5 (75, 87, 89). The yeast CTR recruits the Paf1 complex (45, 89), and the fission yeast CTR binds the capping enzyme (65). Recently, ChIP with microarray technology (ChIP-chip) analysis implicated the CTR in recruiting the histone deacetylase subunit Rco1 (17). The CTR forms a repeat structure similar to the Pol II CTD (77). The *S. cerevisiae* CTR consists of 15 hexapeptide repeats of the consensus sequence S[T/A]WGG[A/Q], (positions where alternative amino acids can occur between different repeats are indicated by brackets, and varying amino acids are indicated by slashes), whereas the human CTR consists of pentapeptide repeats with the consensus sequence GS[R/Q]TP (87) and the fission yeast CTR consists of nonapeptide repeats with the consensus sequence TPAWNSGSK (65).

Deletion of the Spt5 CTR in yeast is not lethal (16, 45, 89) but leads to sensitivity to 6-AU and a slow-growth phenotype at 16°C (45, 89). The CTR deletion is synthetically lethal with the deletion of the gene for the Pol II CTD kinase Ctk1 (45). Deletion of the CTR in fission yeast leads to a slow-growth phenotype and abnormal cell morphology (75). The slow-growth phenotype is intensified if the Pol II CTD is truncated (75), suggesting that the CTR cooperates with the CTD. Deletion of the CTR impairs embryo-

Received 20 September 2011 **Returned for modification** 3 November 2011
Accepted 24 January 2012
Published ahead of print 30 January 2012
Address correspondence to Patrick Cramer, cramer@lmb.uni-muenchen.de.
A.M. and A.S. contributed equally to this article.

doi:10.1128/MCB.06310-11

TABLE 1 Yeast strains used in this study

Strain	Genotype	Source or reference
Wild-type	BY4741; *MAT***a** *his3Δ1 leu2Δ0 met15Δ0 ura3Δ0*	Euroscarf
Wild-type-pRS316	BY4741; pRS316 (URA3)	This study
Bur1-TAP	BY4741; *BUR1*::*TAP*::*HIS3MX6*	Open Biosystems
Clp1-TAP	BY4741; *CLP1*::*TAP*::*HIS3MX6*	This study
Ctk1-TAP	BY4741; *CTK1*::*TAP*::*HIS3MX6*	Open Biosystems
Elf1-TAP	BY4741; *ELF1*::*TAP*::*HIS3MX6*	Open Biosystems
Hrp1-TAP	BY4741; *HRP1*::*TAP*::*HIS3MX6*	This study
Paf1-TAP	BY4741; *PAF1*::*TAP*::*HIS3MX6*	Open Biosystems
Pap1-TAP	BY4741; *PAP1*::*TAP*::*HIS3MX6*	Open Biosystems
Pcf11-TAP	BY4741; *PCF11*::*TAP*::*HIS3MX6*	Open Biosystems
Rna14-TAP	BY4741; *RNA14*::*TAP*::*HIS3MX6*	Open Biosystems
Rna15-TAP	BY4741; *RNA15*::*TAP*::*HIS3MX6*	Open Biosystems
Rpb3-TAP	BY4741; *RPB3*::*TAP*::*HIS3MX6*	Open Biosystems
Spn1-TAP	BY4741; *SPN1*::*TAP*::*HIS3MX6*	Open Biosystems
Spt4-TAP	BY4741; *SPT4*::*TAP*::*HIS3MX6*	Open Biosystems
Spt6-TAP	BY4741; *SPT6*::*TAP*::*HIS3MX6*	Open Biosystems
Spt16-TAP	BY4741; *SPT16*::*TAP*::*HIS3MX6*	Open Biosystems
Spt5 ΔCTR	BY4741; *SPT5Δ931-1063*::*KANMX6*	This study
Spt5 ΔCTR-pRS316	BY4741; *SPT5Δ931-1063*::*KANMX6*; pRS316 [*URA3*]	This study
Bur1-TAP Spt5 ΔCTR	BY4741; *BUR1*::*TAP*::*HIS3MX6 SPT5Δ931-1063*::*KANMX6*	This study
Clp1-TAP Spt5 ΔCTR	BY4741; *CLP1*::*TAP*::*HIS3MX6 SPT5Δ931-1063*::*KANMX6*	This study
Ctk1-TAP Spt5 ΔCTR	BY4741; *CTK1*::*TAP*::*HIS3MX6 SPT5Δ931-1063*::*KANMX6*	This study
Elf1-TAP Spt5 ΔCTR	BY4741; *ELF1*::*TAP*::*HIS3MX6 SPT5Δ931-1063*::*KANMX6*	This study
Hrp1-TAP Spt5 ΔCTR	BY4741; *HRP1*::*TAP*::*HIS3MX6 SPT5Δ931-1063*::*KANMX6*	This study
Paf1-TAP Spt5 ΔCTR	BY4741; *PAF1*::*TAP*::*HIS3MX6 SPT5Δ931-1063*::*KANMX6*	This study
Pap1-TAP Spt5 ΔCTR	BY4741; *PAP1*::*TAP*::*HIS3MX6 SPT5Δ931-1063*::*KANMX6*	This study
Pcf11-TAP Spt5 ΔCTR	BY4741; *PCF11*::*TAP*::*HIS3MX6 SPT5Δ931-1063*::*KANMX6*	This study
Rna14-TAP Spt5 ΔCTR	BY4741; *RNA14*::*TAP*::*HIS3MX6 SPT5Δ931-1063*::*KANMX6*	This study
Rna15-TAP Spt5 ΔCTR	BY4741; *RNA15*::*TAP*::*HIS3MX6 SPT5Δ931-1063*::*KANMX6*	This study
Rpb3-TAP Spt5 ΔCTR	BY4741; *RPB3*::*TAP*::*HIS3MX6 SPT5Δ931-1063*::*KANMX6*	This study
Spn1-TAP Spt5 ΔCTR	BY4741; *SPN1*::*TAP*::*HIS3MX6 SPT5Δ931-1063*::*KANMX6*	This study
Spt4-TAP Spt5 ΔCTR	BY4741; *SPT4*::*TAP*::*HIS3MX6 SPT5Δ931-1063*::*KANMX6*	This study
Spt6-TAP Spt5 ΔCTR	BY4741; *SPT6*::*TAP*::*HIS3MX6 SPT5Δ931-1063*::*KANMX6*	This study
Spt16-TAP Spt5 ΔCTR	BY4741; *SPT16*::*TAP*::*HIS3MX6 SPT5Δ931-1063*::*KANMX6*	This study
rna14-1	*MATα ura3-1 trp1-1 ade2-1 leu2-3 his3-11 rna14-1*	4

genesis in zebrafish and leads to a derepression of gene transcription in zebrafish and human cells (12).

Similar to the Pol II CTD, the CTR of Spt5 can be phosphorylated by the kinases Bur1 and P-TEFb in yeast and humans, respectively (45, 87, 89). CTR phosphorylation promotes transcription elongation in yeast and is important for the cotranscriptional recruitment of the Paf1 complex and for histone modification (45, 89). In human cells, CTR phosphorylation by P-TEFb converts Spt5 from a negative to a positive elongation factor (87). The Spt5 CTR may also play a role in the suppression of transcription-coupled nucleotide excision repair in yeast (16).

Spt5 is also involved in RNA 3′ processing and transcription termination. Processing of mRNA 3′ ends occurs in two steps, endonucleolytic cleavage and the addition of a poly(A) tail (8). In yeast, cleavage and polyadenylation are performed by the complexes cleavage factor I (CFI) and cleavage/polyadenylation factor (CPF) (49). CFI can be separated into CFIA and CFIB (23, 33). CFIA consists of Clp1, Rna14, Rna15, and Pcf11 (4, 57, 58), whereas CFIB consists of Hrp1 (23, 32, 56). Whereas all CFIA subunits have homologs in mammalian cells, no homologs of CFIB are currently known in higher eukaryotes (49).

Here we show that the Spt5 CTR is required for normal recruitment of CFI to the 3′ ends of yeast genes *in vivo* and interacts with CFI *in vitro*. High-resolution genome-wide occupancy profiling of CFI subunits reveals peak occupancy levels about 100 nucleotides (nt) downstream of the pA site. Our results indicate that the Spt5 CTR cooperates with nascent RNA and the serine 2 (S2)-phosphorylated form of the Pol II CTD to recruit CFI to the 3′ ends of genes.

MATERIALS AND METHODS

Yeast strains and phenotyping. *S. cerevisiae* strains containing C-terminally tandem affinity purification (TAP)-tagged versions of target proteins (TAP strains are from Open Biosystems) were used and validated as described earlier (52). The TAP strains were used for deletion of the 15 C-terminal hexapeptide repeats, amino acids 931 to 1063, of Spt5 (89) by homologous recombination with the KanMX6 cassette, amplified from the pFA6a-KanMX6 vector. Table 1 lists all strains used in this study. For growth curve measurements, liquid overnight cultures of wild-type yeast and the strain lacking the Spt5 CTR (residues 931 to 1063; Spt5 ΔCTR) were diluted with yeast extract-peptone-dextrose (YPD) to a starting optical density at 600 nm (OD_{600}) of 0.1. Yeast cells were grown for 18 h, and the OD_{600} was determined every 90 min. Biological triplicate measurements were performed. Growth of wild-type and Spt5 ΔCTR strains was also tested on YPD plates at different temperatures. Cells were grown in YPD at 30°C to stationary phase and diluted to an OD_{600} of ~1.0 with fresh medium. Equal amounts of cells were spotted on YPD plates in

20-fold serial dilutions. Plates were incubated at 16°C, 30°C, or 37°C and inspected daily. To assess potential defects in transcription elongation, wild-type and ΔCTR cells transformed with the pRS316 plasmid containing a *URA* marker were spotted in serial dilutions on SC plates lacking uracil (SC-ura plates) (2% agar, 0.69% yeast nitrogen base, 0.077% dropout ura, 2% glucose; ForMedium) containing 50 μg/ml of 6-AU or 15 μg/ml of mycophenolic acid (MPA) at 30°C.

Chromatin immunoprecipitation. For ChIP experiments, yeast cultures were grown in 40 ml of YPD medium at 30°C to mid-log phase (OD_{600}, ~0.8) and treated with formaldehyde (1%; catalog no. F1635; Sigma) for 20 min at 20°C; cross-linking was quenched with 5 ml of 3 M glycine for 10 min. Subsequent steps were performed at 4°C with precooled buffers containing protease inhibitors (1 mM leupeptin, 2 mM pepstatin A, 100 mM phenylmethylsulfonyl fluoride, 280 mM benzamidine). Cells were collected by centrifugation, washed twice with 1× TBS buffer (20 mM Tris-HCl [pH 7.5], 150 mM NaCl) and twice with FA lysis buffer (50 mM HEPES-KOH [*N*-2-hydroxyethylpiperazine-*N*′-2-ethanesulfonic acid–potassium hydroxide] [pH 7.5], 150 mM NaCl, 1 mM EDTA, 1% Triton X-100, 0.1% sodium deoxycholate, 0.1% SDS). Cell pellets were flash frozen in liquid nitrogen and stored at −80°C. Pellets were thawed, resuspended in 1 ml of FA lysis buffer, and disrupted by bead beating (Retsch) in the presence of 1 ml of silica-zirconium beads for 30 min at 4°C. Lysis efficiency was typically >80%. Chromatin was solubilized and fragmented via sonication with a Bioruptor UCD-200 instrument (Diagenode, Inc.). Seven hundred microliters of the sample was immunoprecipitated with 20 μl of IgG-Sepharose 6 Fast Flow beads (GE Healthcare) at 4°C for 1 h. The IgG beads were directed against the protein A content of the C-terminal TAP tag. Immunoprecipitated chromatin was washed three times with FA lysis buffer, twice with FA lysis buffer containing 500 mM mM NaCl, twice with ChIP wash buffer (10 mM Tris-HCl [pH 8.0], 0.25 M LiCl, 1 mM EDTA, 0.5% NP-40, 0.5% sodium deoxycholate), and once with TE buffer (10 mM Tris-HCl [pH 7.4], 1 mM EDTA). Immunoprecipitated chromatin was eluted for 10 min at 65°C with ChIP elution buffer (50 mM Tris-HCl [pH 7.5], 10 mM EDTA, 1% SDS). Eluted chromatin was digested with proteinase K (Sigma) at 37°C for 2 h, and the reversal of cross-links was performed at 65°C overnight. DNA was purified with a QIAquick PCR purification kit (Qiagen) according to the manufacturer's instructions. An RNase-ChIP assay was performed as described previously (1). Briefly, the following adaptations to the ChIP protocol were made. First, the cross-linking time was reduced to 5 min. Second, the chromatin solution was divided into two samples before the immunoprecipitation (IP) step. One chromatin sample was treated with 7.5 U of RNase A and 300 U of RNase T1 (Ambion); the other sample was treated with the same volume of the RNase storage buffer (10 mM HEPES [pH 7.5], 20 mM NaCl, 0.1% Triton X-100, 1 mM EDTA, 50% glycerol [vol/vol]). After a 30-min incubation at room temperature, IP was performed as above.

ChIP-chip occupancy profiling. ChIP-chip experiments were performed and analyzed as described previously (52). Briefly, ChIP-chip data for TAP-tagged factors were normalized using both mock immunoprecipitation and input measurements. The normalized signal was converted to occupancy values between 0% and 100% by setting the genome-wide 99.8% quantile to 100% occupancy and the 10% quantile to 0% occupancy. For the Rpb3 profiles in the wild-type and Spt5 ΔCTR backgrounds, ChIP enrichments were obtained by dividing ChIP intensities by the genomic input intensities. The normalized occupancy or enrichment signal at each nucleotide was calculated as the median signal for all probes overlapping this position. Profiles were smoothed using running median smoothing with a window half size of 75 bp. To average profiles over genes, we filtered yeast genes. Of 4,366 yeast genes with annotated transcriptional start sites (TSS) and pA sites (61), the 50% most highly expressed genes (14) that were at least 200 nt away from neighboring genes (all-gene set, 1,140 genes) were examined. Three open reading frame (ORF)-length classes were defined, short (S; 512 to 937 bp), medium (M; 938 to 1,537 bp), and long (L; 1,538 to 2,895 bp), comprising 266, 339, and 299 filtered genes, respectively. Profiles within these groups were scaled to median gene length, and the gene-averaged profiles were calculated by taking the median over genes at each genomic position.

Quantitative real-time PCR. Input and immunoprecipitated samples were assayed by quantitative real-time PCR (qPCR) to assess the extent of protein occupancy at different genomic regions. Primer pairs directed against the transcriptional start site, coding, pA, and 3′ regions of the *ADH1*, *ILV5*, *PDC1*, and *TEF1* genes as well as against a heterochromatic control region of chromosome V were used to determine PCR efficiencies. All PCR efficiencies ranged between 95% and 100%. The PCR mixtures contained 1 μl of DNA template, 2 μl of 10 μM primer pairs, and 12.5 μl of iTaq SYBR green supermix (Bio-Rad). qPCR was performed on a Bio-Rad CFX96 real-time system (Bio-Rad Laboratories, Inc.) using a 3-min denaturing step at 95°C, followed by 49 cycles of 30 s at 95°C, 30 s at 61°C, and 15 s at 72°C. Threshold cycle (C_T) values were determined by application of the corresponding Bio-Rad CFX Manager software, version 1.1, using the C_T determination mode "Regression." The fold enrichment of any given region over an ORF-free heterochromatic region on chromosome V was determined as described previously (19). The RNase ChIP data for Rna14 (data not shown) and Rna15 were further analyzed as follows. The calculated fold enrichment values of the gene region for the different biological replicates were averaged. The fold enrichment values of chromatin samples that were not treated with the RNase mix were averaged and set to 100%. Sequence information for the primer pairs used in this study is available upon request.

Rapid amplification of cDNA 3′ ends. For RNA isolation, overnight yeast cultures grown from four different wild-type and Spt5 ΔCTR colonies were diluted in 20 ml of fresh YPD medium to an OD_{600} of ~0.1 and grown at 30°C to mid-log phase (OD_{600}, ~0.8). A RiboPure yeast kit (Applied Biosystems) was used to isolate yeast RNA according to the manufacturer's instructions. Rapid amplification of cDNA 3′ ends (3′-RACE) was performed for the *ACT1* gene as described previously (20). This gene was shown to possess several alternative pA sites and was used in 3′-end-processing studies (3, 48). The *ACT1* cDNA was synthesized as described previously (3) using SuperScript II reverse transcriptase (Invitrogen), 0.5 μM anchored oligo(dT) primer containing an XhoI restriction site, underlined in the sequence 5′-GACTCGAGTCGACATCGATTTTTTTTTTTTTTTT-3′, and 2 μg of RNA template. Next, RNA was digested using RNase H (New England BioLabs, Inc.) for 20 min at 37°C. The enzyme was inactivated by incubation at 65°C for 20 min. PCRs were conducted using the cDNA samples, 0.25 μM gene-specific upstream primer containing an EcoRI restriction site (underlined in the sequence 5′-TATGAATTCTTCTGTTTTGGGTTTGGA-3′), an anchored primer (5′-GACTCGAGTCGACATCGA-3′; an XhoI restriction site is underlined), and *Taq* DNA polymerase (Fermentas; Thermo Fisher Scientific). The PCR product and the pET28b vector were digested with EcoRI-HF as well as XhoI (New England BioLabs, Inc.) and then ligated and transformed into competent *Escherichia coli* XL1-Blue cells (Stratagene; Agilent Technologies). Plasmids from 22 *E. coli* colonies derived from wild-type and 24 colonies derived from Spt5 ΔCTR clones, respectively, were sequenced (GATC Biotech) using pET28b sequencing primers (forward, 5′-TAATACGACTCACTATAGGG-3′; reverse, 5′-GGGTTATGCTAGTTATTGC-3′).

Pol II readthrough assay. The readthrough was performed for the *PMA1* gene according to the method of Ahn et al. (3) using a gene-specific forward primer (5′-CTATTATTGATGCTTTGAAGACCTCCAG-3′) and two reverse primers positioned at different regions downstream of the transcription termination site (first primer, 5′-CAAGAAAGAAAAAGTACCATCCAGAG-3′; second primer, 5′-GTAAATTTGTATACGTTCATGTAAGTG-3′). RNA isolation, reverse transcription, and PCR were conducted as described above, and the PCR products for the wild type and Spt5 ΔCTR mutant were compared by standard agarose gel electrophoresis. Preparation of RNA from the rna14-1 temperature-sensitive mutant was performed as described before but with the following modifications. Yeast cultures were either grown at 24°C to mid-log phase before RNA

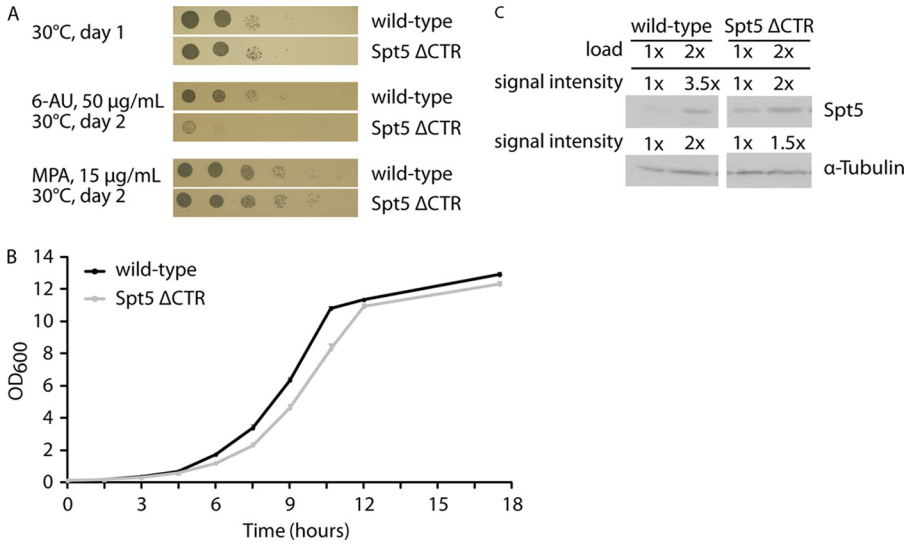

FIG 1 Spt5 CTR deletion leads to a growth defect in the presence of 6-AU and to a slight increase in Spt5 protein levels. (A) The Spt5 ΔCTR mutant shows a strong growth defect in the presence of 50 μg/ml of 6-AU compared to the wild type. No effects are observed at 30°C or 37°C (data not shown) or in the presence of 15 μg/ml of mycophenolic acid (MPA) on solid medium. (B) The Spt5 ΔCTR mutant grown in liquid YPD medium shows a slight growth defect at 30°C compared to the wild type. The standard deviations for three independent measurements are indicated for each data point. (C) Spt5 protein levels in the ΔCTR mutant are upregulated 1.7-fold compared to those of the wild type. Quantitative Western blotting was performed with antibodies against Spt5 and α-tubulin. Different amounts of protein were loaded, and quantification of the intensities was performed. Normalization of the Spt5/α-tubulin ratio obtained for Spt5 ΔCTR cells against the corresponding ratio of wild-type cells revealed that Spt5 protein levels were slightly elevated (1.7-fold) in cells lacking the CTR of Spt5.

isolation (see Fig. 6B, rna14-1 24°C) or grown to an OD_{600} of ~0.8 at 24°C and then transferred to 37°C (restrictive temperature) for 1 h (see Fig. 6B, rna14-1 37°C) before RNA was prepared.

GST pulldown assay. To prepare yeast cell lysates, we performed cell lysis as for ChIP experiments but with the following modifications: (i) cell cultures were grown in 200 ml of YPD medium at 30°C but not cross-linked with formaldehyde, and (ii) cell debris was removed by centrifugation. A synthetic DNA construct of the glutathione *S*-transferase (GST) tag based on the pGEX3T vector fused to the DNA sequence coding for Spt5 CTR residues 931 to 1063 (89) was synthesized (Mr. Gene GmbH; sequence available upon request) and cloned into vector pET28b. Expression of the GST-Spt5CTR fusion construct (pET28b) and the GST tag alone (pGEX-4T-1) in *E. coli* was induced with 0.5 mM IPTG (isopropyl-β-D-thiogalactopyranoside) at 18°C overnight in 1-liter cultures. Cells were lysed by sonification in 50 ml of lysis buffer (50 mM Tris [pH 8.0], 150 mM NaCl, 1 mM dithiothreitol [DTT], and protease inhibitors; see ChIP protocol) for 15 min (Branson 250 sonifier instrument). The cell debris was removed by centrifugation. For pulldown experiments, *E. coli* cell lysates were incubated with 100 μl of glutathione-Sepharose beads (GE Healthcare) preequilibrated in lysis buffer for 1 h at 4°C. Beads were washed eight times with lysis buffer and incubated for 1 h at room temperature with 300 μl of yeast cell lysate prepared from yeast strains that express TAP-tagged versions of CFI subunits. Next, beads were washed eight times with lysis buffer and proteins were eluted from the beads eight times with lysis buffer containing 10 mM glutathione. All elution fractions were pooled, and the protein was precipitated with 10% trichloroacetic acid (TCA). The protein pellet was washed with ice-cold acetone and resuspended in 2× SDS-PAGE loading buffer (5% glycerol, 25 mM Tris [pH 7.0], 0.05% bromophenol blue, 0.5% β-mercaptoethanol, 7% DTT, 0.05% lauryl sulfate). Wash and elution fractions were analyzed by SDS-PAGE and Western blotting with antibodies against the TAP tag of CFI subunits (peroxidase antiperoxidase [PAP]; catalog no. P1291; Sigma-Aldrich) and the GST tag (RPN1236; GE Healthcare).

Western blot analysis. For TAP strain validation, total protein samples were generated directly from single colonies according to the method of Knop et al. (37) with minor modifications. After SDS-PAGE, samples were blotted onto a polyvinylidene difluoride (PVDF) membrane (Roth) and the membrane was probed with the primary antibody against the TAP tag (PAP; catalog no. P1291; Sigma-Aldrich). Antibody detection was performed using Pierce enhanced chemiluminescence (ECL) Western blotting substrate (Thermo Scientific) and Amersham Hyperfilm ECL (GE Healthcare). Quantification of the Spt5 protein levels in wild-type and Spt5 ΔCTR cells was performed using one time and two times the amounts of total protein samples from the wild type and Spt5 ΔCTR mutant to ensure the linearity of the antibody signal quantification. Signals were quantified using an antibody against the N terminus of Spt5 (yN-20; catalog no. sc-26355; Santa Cruz) and the α-tubulin antibody (3H3087; catalog no. sc-69971; Santa Cruz). The antibody signal was detected quantitatively using Pierce ECL Western blotting substrate and a LAS-3000 camera (Fujifilm). Spt5 protein signals were quantified relative to the α-tubulin signals using ImageQuant 5.0 software (GE Healthcare). For evaluation of the GST pulldown experiments, the membrane was probed with the PAP antibody against the TAP tag of Rna14 (PAP; catalog no. P1291; Sigma-Aldrich) and the GST antibody (RPN1236; GE Healthcare).

Microarray data accession number. Raw and normalized data are available at Array Express under accession number E-TABM-1225.

RESULTS

Investigation of elongation factor recruitment by Spt5 CTR. To investigate whether the function of the yeast Spt5 CTR in recruiting Pol II-associated factors extends to elongation factors other than Paf1 (45, 89), we carried out ChIP analysis in strains lacking the Spt5 CTR. We generated a yeast strain with a CTR deletion (see Materials and Methods). As reported previously, CTR deletion led to sensitivity to 6-AU and a slow-growth phenotype at 16°C (Fig. 1A) (45, 89). We also observed a slight growth defect at 30°C (Fig. 1B), but not at 37°C (data not shown). In contrast to observations of *S. pombe* (75), the morphology of *S. cerevisiae* was not altered

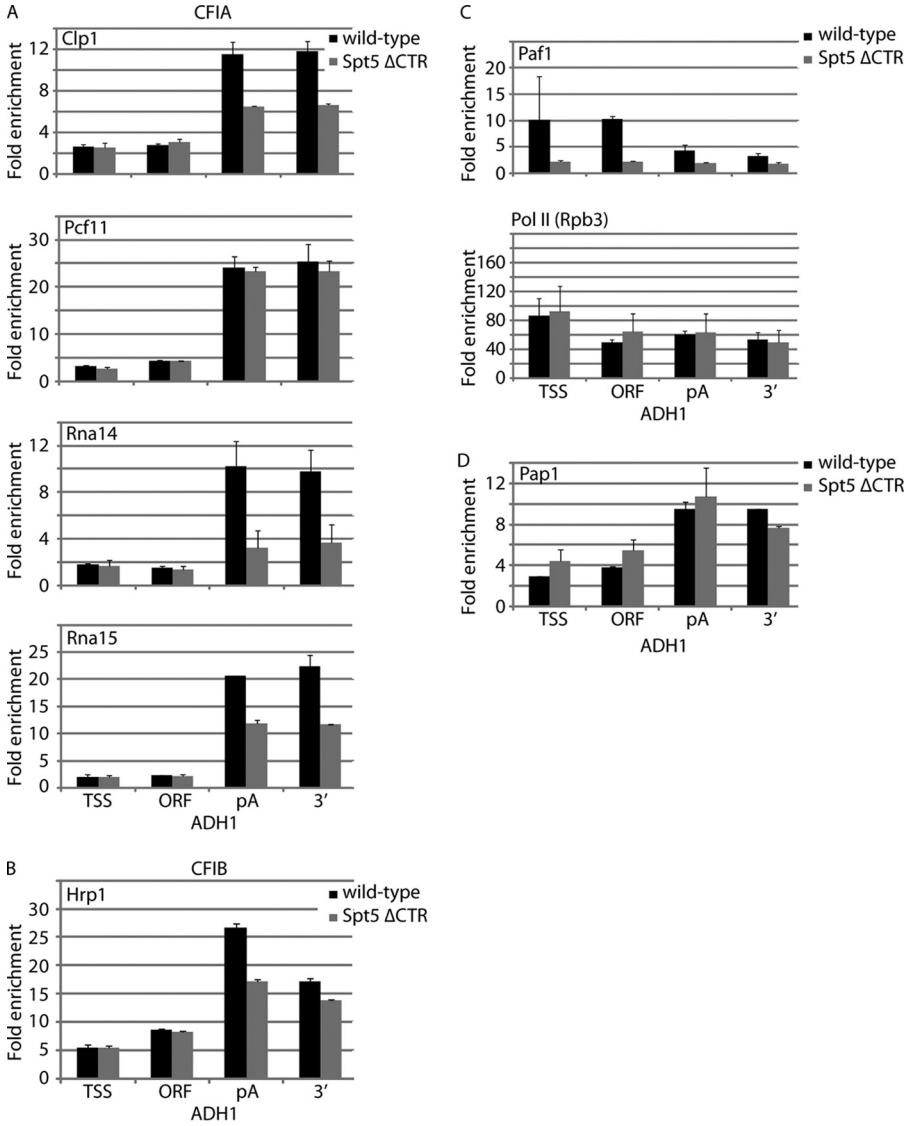

FIG 2 ChIP analysis reveals that CFI occupancy is reduced in Spt5 ΔCTR cells. This is true for CFIA subunits (A), except for Pcf11, as well as for CFIB/Hrp1 (B). (C) Whereas Paf1 occupancy, as determined by ChIP, is strongly reduced in Spt5 ΔCTR cells, Pol II levels are not affected. (D) Pap1 occupancy is not changed in Spt5 ΔCTR cells. The fold enrichments at the *ADH1* gene over a nontranscribed region that is located near the centromere of chromosome V are given for the TSS, the ORF region, the pA site, and the region 3′ of the pA site. ChIP-determined occupancies are indicated for wild-type and Spt5 ΔCTR cells as black and gray bars, respectively. The standard deviations are for at least two independent ChIP experiments.

upon CTR deletion (data not shown). Quantitative Western blot analysis revealed approximately 1.7-fold-higher Spt5 protein levels in cells lacking the CTR (Fig. 1C).

For ChIP analysis, we fused a TAP tag to the C terminus of elongation factors in the CTR deletion background. The occupancy levels of the elongation factors were determined by ChIP at different positions of genes *ADH1*, *ILV5*, *PDC1*, and *TEF1*. We chose these genes for several reasons. First, these genes encode housekeeping proteins, are highly expressed (14), and are heavily occupied by Pol II in the mid-log phase of yeast growth (52). Second, their DNA elements, including the TSS and the pA site, are well characterized (13, 35, 61). Third, the transcription unit is long enough to distinguish between different binding levels at distinct positions of the gene.

We performed ChIP analyses for eight Pol II elongation factors that belong to the three different groups described recently (52): (i) Spt4 and Spt6 (group 1), (ii) Elf1 and Spn1 (group 2), and (iii) Bur1, Ctk1, Paf1, and Spt16 (group 3). The results are shown only for Paf1 (Fig. 2C). These data revealed strong factor binding at the *ADH1* gene. A severe decrease in Paf1 occupancy to about 20% was detected at the *ADH1* gene (Fig. 2C), consistent with previous reports (45, 89) and providing a positive control. The difference in Paf1 occupancy was not due to a difference in Pol II occupancy, which was unaffected by CTR deletion (Fig. 2C). However, the other representative elongation factors tested did not show significant differences in their gene occupancies (data not shown), indicating that CTR deletions specifically reduce the gene occupancy of Paf1.

Spt5 CTR is required for recruitment of CFI *in vivo*. Since Spt5 colocalizes with 3′-end-processing factors (35, 52, 81) and

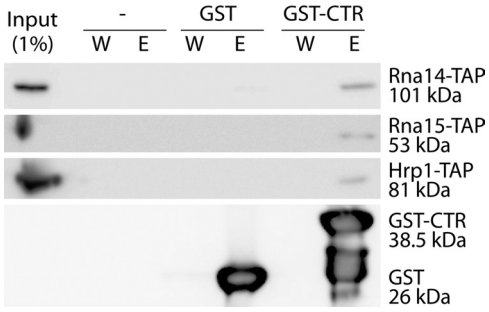

FIG 3 The Spt5 CTR interacts with CFI subunits *in vitro*. GST pulldown experiments were performed with a GST-Spt5 CTR fusion protein (GST-CTR), with GST alone (GST), and without protein (−), which served as a negative control. Western blotting was performed for the last washing fractions (W), the combined elution fractions (E) of the samples, and 1% of the Rna14-TAP (first panel), Rna15-TAP (second panel), and Hrp1-TAP (third panel) yeast cell lysates (Input) with antibodies against the TAP tag of the corresponding CFI subunit and the GST tag (for details, see Materials and Methods). The signals obtained for GST and GST-CTR were similar and are exemplarily shown for the pulldown experiments with Rna14-TAP (fourth panel).

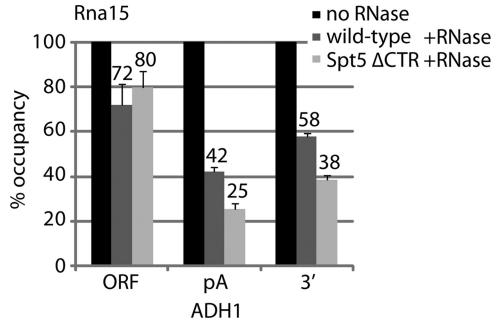

FIG 4 RNase-ChIP assays reveal that RNA contributes to CFI recruitment in Spt5 ΔCTR cells. RNA-dependent binding is given for the ORF region, the pA site, and a region 3′ of the pA site of the *ADH1* gene. The ChIP occupancy signal of Rna15 without RNase treatment was set to 100%. The relative ChIP signals of Rna15 for wild-type and Spt5 ΔCTR cells after RNase treatment are indicated. The corresponding percentages are given above the bars. Standard deviations were calculated from four independent experiments.

copurifies with these factors (44), we tested whether it plays a role in the recruitment of 3′-end-processing and transcription termination factors. ChIP analysis revealed that all CFIA subunits, Clp1, Pcf11, Rna14, and Rna15, showed high occupancy at the 3′ ends of protein-coding genes and the pA sites (Fig. 2A). In Spt5 ΔCTR cells, occupancy of Clp1, Rna14, and Rna15 was reduced more than 50% at the *ADH1* gene and was also markedly lower at other tested genes (data not shown). However, we observed no difference between wild-type yeast and Spt5 ΔCTR cells in the occupancy of Pcf11 (Fig. 2A).

Since CFIA is associated with CFIB/Hrp1, we investigated whether Hrp1 occupancy was affected by CTR deletion. Previous ChIP analyses have shown that Hrp1 cross-links throughout the coding regions to the 3′ ends of genes (35, 39). Our ChIP analysis revealed that Hrp1 shows the strongest level of occupancy near the pA site, although it is recruited earlier than CFIA subunits (Fig. 2B). Similar to the occupancy of CFIA subunits, Hrp1 binding was markedly reduced in Spt5 ΔCTR cells (Fig. 2B). However, no occupancy difference could be observed for the poly(A) polymerase Pap1 (Fig. 2D), which is also required for 3′ end processing (49, 55). Taken together, these findings show that the Spt5 CTR plays a crucial role in the recruitment of CFI, but not of Pap1, to the 3′ ends of protein-coding genes.

Spt5 CTR interacts with CFI *in vitro*. Since CFI recruitment to genes was impaired upon CTR deletion, we asked whether the Spt5 CTR interacts with CFI *in vitro*. We performed pulldown experiments with a recombinantly expressed GST-tagged version of the Spt5 CTR and yeast cell lysates prepared from strains that expressed TAP-tagged versions of CFI subunits. Western blot analysis of the eluates with antibodies directed against the GST tag and the TAP tag of each CFI subunit revealed coprecipitation of the GST-tagged Spt5 CTR and the CFI subunits Rna14, Rna15, and Hrp1, but there was no interaction with GST alone (Fig. 3). Coprecipitation could not be detected for Pcf11 (data not shown), in agreement with the ChIP data that showed that Pcf11 occupancy is not altered in Spt5 ΔCTR cells (Fig. 2A). For Clp1, the input signal in the Western blot analysis was much lower than those for other CFI subunits, such that a possible interaction between the Spt5 CTR and Clp1 cannot be ruled out. Taken together, these pulldown experiments revealed a previously unobserved interaction between the Spt5 CTR and CFI *in vitro*. Since the interaction was detected with the use of a lysate that naturally contains many nonspecific competitor proteins, and since it was not observed with the GST tag alone, it must be regarded as being highly specific. It is possible, however, that the interaction is mediated by other proteins in the extract and is thus indirect.

RNA contributes to CFI recruitment. Since deletion of the Spt5 CTR led to a marked reduction in the occupancy of CFI subunits, but not to a complete loss, we asked which factors contribute to the residual binding of CFI. Since Rna15 and Hrp1 contain RNA recognition motifs that are known to bind RNA sequences *in vitro* (33, 41, 63, 67), we reasoned that nascent RNA may contribute to CFI recruitment. To address this, we performed an RNase-ChIP assay (1). In this assay, RNA is digested before the immunoprecipitation step, leading to a drop in factor occupancy if factor recruitment involves RNA.

We performed RNase-ChIP for Rna15 (Fig. 4) and Rna14 (data not shown). First, we observed a decrease in Rna15 occupancy after RNase treatment, indicating an important role of RNA in Rna15 recruitment, both in wild-type and Spt5 ΔCTR cells. Second, Rna15 binding most strongly depended on RNA around the pA site of the *ADH1* gene. Third, the strongest reduction in Rna15 occupancy was observed when both the Spt5 CTR was deleted and the RNA was removed by RNase treatment. The additional decrease in the Rna15 occupancy level was highly reproducible and could be observed in all four independent biological replicates. A similar RNA dependence could be observed for Rna14 (data not shown). These results indicate that RNA contributes to CFI recruitment *in vivo* and that this can explain the residual recruitment of CFI in cells lacking the Spt5 CTR.

CFI colocalizes with the S2-phosphorylated CTD downstream of the pA site. It has been shown for mammalian cells that homologs of the yeast CFI complex are already recruited at the promoter regions of genes (22, 79). One study in yeast showed that some RNA 3′-end-processing factors, including Rna14 and Rna15, also cross-linked to the promoter and the early coding region of the *PMA1* gene, but not to other genes tested (35). However, our ChIP analysis (Fig. 2) and published data for yeast (35,

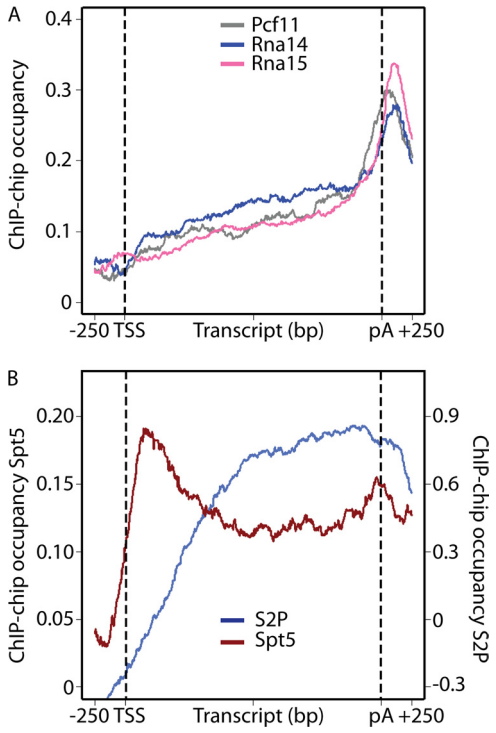

FIG 5 Genome-wide ChIP-chip occupancy profiling of CFI subunits in yeast. (A) Gene-averaged profiles for the long-gene-length class (2,350 ± 750 nt, 299 genes; see Materials and Methods) for Pcf11 (52), Rna14, and Rna15. Profiles of other length classes are generally similar (data not shown). Dashed black lines indicate the TSS and pA site. (B) Gene-averaged profiles as for panel A for the transcription elongation factor Spt5 (52) and the S2-phosphorylated (S2P) CTD form of Pol II (52). Occupancies and signal intensities are given for Spt5 and the S2-phosphorylated form of Pol II on the left and right *y* axes, respectively.

43) suggest that CFI subunits cross-linked near the pA site at the 3′ ends of genes.

To investigate the preferred location of CFI subunits on a genome-wide level, we performed ChIP-chip analysis for Rna14 and Rna15. This revealed CFI recruitment at all protein-coding genes that are occupied by Pol II and its elongation factors (52). The ChIP-chip profiles showed sharp occupancy peaks for Rna14 and Rna15 105 nt and 108 nt downstream of the pA site, respectively (Fig. 5A). We also detected weak Rna14 and Rna15 binding over the transcribed region, with an increase toward the 3′ end. These profiles were independent of gene length (Fig. 4A and data not shown). Comparison with previous profiles (Fig. 5A) (52) revealed that the peak occupancies of Rna14 and Rna15 coincided with Pcf11 occupancy, which peaked 52 nt downstream of the pA site (Fig. 5A). Further, CFI subunit peak occupancies occurred in a region where the occupancies for Spt5 and the S2-phosphorylated Pol II were high (Fig. 5B). The sharp occupancy drop-off of CFI subunits coincided with the drop-off for the ChIP signal of the S2-phosphorylated CTD, consistent with its role in CFI recruitment.

CTR deletion does not impair termination. Previous studies showed that mutations in Pcf11, Rna14, and Rna15 can lead to defects in transcript cleavage and readthrough transcription beyond the termination site (6, 9, 71). Therefore, we investigated whether the reduced level of CFI recruitment observed in Spt5 ΔCTR cells leads to Pol II readthrough transcription at the *ACT1*, *PMA1*, and *RNA14* genes. To detect transcriptional readthrough, we chose a PCR-based method with a gene-specific forward primer and different reverse primers positioned downstream of the normal transcript termination site, as described previously (3) (Fig. 6A). In this assay, a prolonged transcript resulting from readthrough transcription would be detected by the generation of PCR products with a reverse primer that is located downstream of the termination site. As shown in Fig. 6B, transcriptional readthrough could be detected when the function of Rna14 was impaired with the use of a temperature-sensitive yeast strain serving as a positive control for this assay. However, no differences in the PCR products, and thus the length of the *PMA1* transcripts, were observed between wild-type and ΔCTR cells (Fig. 6B). Similar results were obtained for the *ACT1* and *RNA14* genes (data not shown). Thus, deletion of the Spt5 CTR does not result in a termination defect that would be detected by transcriptional readthrough.

Although we did not detect readthrough transcription at tested single genes, it may still occur at other genes. To investigate this, we measured high-resolution ChIP-chip occupancy profiles for the Pol II core subunit Rpb3 in wild-type and mutant yeast cells lacking the CTR. The high correlation between the Pol II profiles (Pearson $R = 0.89$) and the high level of similarity of the gene-averaged profiles (Fig. 6C), however, indicated that there is no difference in Pol II occupancy between wild-type and mutant cells. In addition, a difference profile calculated from Rpb3 occupancy in ΔCTR and wild-type cells did not reveal any clusters of altered occupancy. These results show that transcription readthrough does not occur in the ΔCTR strain.

CTR deletion does not alter pA site usage. Since mutations of 3′ end-processing factors were also shown to result in the usage of alternative pA sites (48), we investigated whether CTR deletion and the resulting reduction in CFI recruitment lead to alternative pA site usage. To detect a possible change in the usage of pA sites *in vivo*, we used 3′-RACE, which allows the mapping of the 3′ ends of transcripts (20). We performed 3′-RACE for the *ACT1* and *PMA1* genes, which possess five and two pA sites, respectively (Fig. 6D) (35, 48). The experiments revealed multiple pA sites for the *ACT1* gene, which map to a distinct region at the 3′ end of the gene, 1,508 to 1,617 nt from the TSS. We also quantified the usage of the different pA sites by sequencing at least 22 PCR products from both wild-type and Spt5 ΔCTR clones (see Materials and Methods). For *ACT1*, these experiments revealed three major pA sites that were used in 75% of the cases and six minor pA sites (Fig. 6D). However, no significant difference in pA site usage was detected between wild-type and Spt5 ΔCTR cells (Fig. 6D). Similar results were obtained for the *PMA1* gene (data not shown). Thus, a reduced level of CFI recruitment in Spt5 ΔCTR cells does not lead to altered pA site usage *in vivo*.

DISCUSSION

Two major transitions occur during the Pol II transcription cycle, the initiation-elongation transition at the 5′ ends of genes and the elongation-termination transition at the 3′ ends of genes, which is coupled to 3′ RNA processing. Whereas the first transition has been extensively studied (2, 21, 39, 40, 47, 52, 68), less is known about the second transition. Studies of the second transition revealed a role of the S2-phosphorylated Pol II CTD in the recruitment of 3′-end-processing and termination factors (3, 43, 47, 53, 88). This transition also involves the Paf1 complex (28, 60, 62),

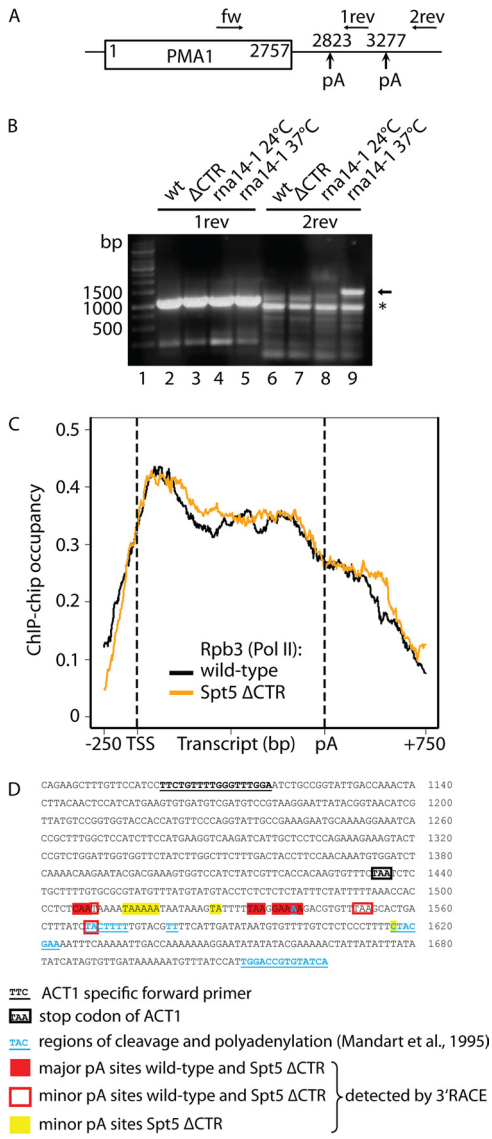

FIG 6 Spt5 CTR deletion provokes neither transcriptional readthrough of Pol II nor alternative pA site usage. (A) Schematic representation of the yeast *PMA1* locus. The ORF region and the two pA sites according to Ahn et al. (3) are indicated by a box and vertical arrows, respectively. The forward primer (fw) and two reverse primers (1-rev and 2-rev) that were used for Pol II readthrough detection are depicted as horizontal arrows. (B) Agarose gel electrophoresis of the five PCR products as described for panel A for the wild type (wt), Spt5 ΔCTR cells (ΔCTR), and the *rna14-1* temperature-sensitive strain grown at permissive (24°C) and restrictive (37°C) temperatures. The *rna14-1* mutant led to a readthrough transcript at 37°C (1.5 kb; black arrow) and served as a positive control. No differences in the lengths of the PCR products could be detected between wild-type and Spt5 ΔCTR cells. The unspecific PCR product also obtained with the second reverse primer (2-rev) is marked by an asterisk. The heights of the marker lanes in base pairs (bp) are shown on lane 1. (C) Gene-averaged occupancy profiles as in Fig. 5 but for the medium-gene-length class (1,238 ± 300 nt, 339 genes; see Materials and Methods) of Pol II (Rpb3) in wild-type and Spt5 ΔCTR cells. (D) The nucleotide sequence of the 3′ region of yeast *ACT1* is shown. Key sequence elements are labeled. 3′-RACE revealed three major RNA cleavage and pA sites (red-filled boxes), site 1 (1,506 nt downstream of start codon ATG; seven and three sequenced clones for the wild-type and Spt5 ΔCTR mutant, respectively), site 2 (1,534 nt downstream of start codon ATG; four and nine sequenced clones, respectively), and site 3 (1,538 nt downstream of start codon ATG; six and five sequenced clones, respectively), and three minor pA sites (red frames), site 1 (1,509 nt downstream of the start codon ATG; one and two sequenced clones for the wild type and Spt5 ΔCTR mutant, respectively) and sites 2 and 3 (1,551 and 1,568 nt downstream of the start codon ATG; two and one sequenced clones, respectively) that were used equally in wild-type and Spt5 ΔCTR cells. Additionally, 3′-RACE led to the mapping of three rare pA sites that were used exclusively in Spt5 ΔCTR cells (yellow boxes; one sequenced clone for each site). For further details, see Materials and Methods.

elongation factor Spt6 (30), and the transcription regulator Sin1 (25).

Here we provide evidence for a role of the Spt5 CTR in the elongation-termination transition, in particular in the recruitment of the essential mRNA 3′-end-processing factor CFI. ChIP analysis of wild-type and Spt5 ΔCTR in yeast cells detected a reduction in the occupancy of Paf1, as described previously (45, 89), but also of CFI subunits, indicating impaired CFI recruitment to the 3′ ends of genes *in vivo*. A pulldown assay additionally revealed an interaction between CFI subunits and the Spt5 CTR *in vitro*. This is consistent with a study showing that Rna14 can be copurified with Spt5 (44). RNase-ChIP experiments for CFI subunits Rna14 and Rna15 showed that RNA contributes to CFI recruitment *in vivo*. Genome-wide profiling by ChIP-chip revealed a sharp peak in Rna14 and Rna15 occupancy around 100 nt downstream of the pA site, which coincides with high occupancy of Spt5 and the S2-phosphorylated Pol II. These results show that the Spt5 CTR contributes to the recruitment of CFI to a defined region at the 3′ ends of yeast genes.

There is evidence that recruitment of RNA 3′-end-processing factors also involves the Paf1 complex (Paf1C). Deletion of subunits of Paf1C reduces the recruitment of Pcf11 (60) and interferes with Pol II binding of Cft1 (62), a component of the yeast CPF complex. Since Paf1 occupancy levels are markedly reduced in Spt5 ΔCTR cells, it may be argued that recruitment of CFI may occur via Paf1C and that the observed reduction in CFI subunit occupancy may result from a loss of Paf1C. However, several lines of evidence argue against this model and instead argue that CFI recruitment occurs via a direct interaction with the CTR. First, Pcf11 occupancy is not altered in Spt5 ΔCTR cells, despite the loss of Paf1C (Fig. 2A and C). Second, despite extensive interactomics studies, physical interactions between Paf1C and CFI have never been observed. Third, Paf1C clearly dissociates from the Pol II elongation complex upstream of the pA site (15, 35, 52), whereas CFI subunits are mainly recruited downstream of the pA site (Fig. 5) (15, 35, 52). These results argue for a Paf1C-independent mechanism of CFI recruitment in yeast.

We further showed that the Spt5 CTR is not required for normal pA site usage and transciption termination *in vivo*. This is consistent with the nonessential nature of the Spt5 CTR in yeast and may be due to residual CFI recruitment in Spt5 ΔCTR cells that likely results from binding of the CFI subunits to RNA and from the binding of Pcf11 to the Pol II CTD. Pcf11 contains an essential CTD interaction domain (CID), which directly binds the S2-phosphorylated CTD (43, 53, 73) and may be responsible for normal recruitment of Pcf11 to genes upon CTR deletion. These observations indicate that CFI is recruited to a defined region downstream of the pA site by simultaneous interactions with the Spt5 CTR, nascent RNA, and the Pol II CTD (Fig. 7). This model is consistent with the reported binding of Rna14 and Rna15 to the phosphorylated CTD (7) and with other published data. Rna15 can be cross-linked to RNA (33) and contains an RNA recognition

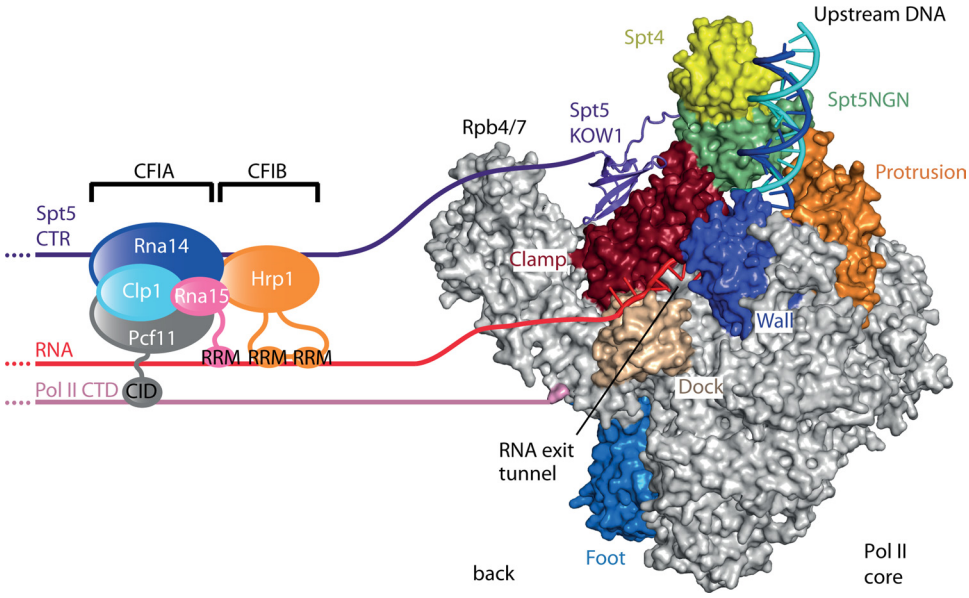

FIG 7 Model of CFI recruitment in yeast. The complete yeast Pol II elongation complex with bound Spt4/5 is viewed from the back (51). Pol II and Spt4/5 are shown as molecular surfaces with key domains highlighted in color and labeled. Exiting RNA, the C-terminal KOW domains, the CTR of Spt5, and the Pol II CTD extend from Pol II around the Rpb4/7 subcomplex, establishing a main interface for CFI recruitment. Rna14 may directly contact the Spt5 CTR, whereas the RNA is bound by the C-terminal RRM domain of Rna15 and by two internal RRM domains of Hrp1. The Pol II CTD is bound by the N-terminal CID domain of Pcf11. CFI subunits are drawn to scale. Important protein domains are illustrated as extensions from the protein cores.

motif (RRM) domain that binds GU-rich RNA (41, 63). Hrp1 has two RRMs that bind to AU-containing RNAs (67).

Finally, our results have implications for understanding the evolution of transcription-coupled events. Spt5 represents the only known RNA polymerase-associated factor that is conserved in all three domains of life (85); its bacterial homolog is called NusG (24). All Spt5 homologs contain two conserved domains, the NusG N-terminal domain (NGN) and a C-terminal KOW domain (26). Whereas the NGN domain binds to the polymerase clamp domain and closes the active center cleft, apparently to render transcription processive, the KOW domain extends from the polymerase surface toward exiting RNA (36, 51, 59) (Fig. 7). In bacteria, the KOW domain interacts with the ribosome, thus coupling transcription to mRNA translation (11, 70). In eukaryotes, transcription and translation take place in different cellular compartments, and any coupling between these processes would likely occur via the mRNA that exits the nucleus (27, 50). Our data indicate that the CTR of Spt5 contributes to the coordination of transcription with 3′ RNA processing, which in turn is coupled to mRNA export (29, 46, 72). Since the CTR occurs only in eukaryotic Spt5 homologs, it is likely that it emerged during evolution to maintain coupling between transcription and translation after the spatial separation of these processes. Such coupling may be achieved by cotranscriptional Spt5-dependent loading of mRNA export factors onto the nascent RNA, before its maturation, nuclear export, and translation in the cytosol.

ACKNOWLEDGMENTS

We thank K. Maier for help with generating the original Spt5 ΔCTR strain and A. Meinhart (Max Planck Institute for Medical Research, Heidelberg) for advice. We thank M. Kim (Seoul National University) for providing the rna14-1 temperature-sensitive yeast strain.

This work was supported by grants from the Deutsche Forschungsgemeinschaft (SFB646, TR5, FOR1068, and NIM), the European Molecular Biology Organization (EMBO), the Boehringer Ingelheim Fonds, the Elite Network of Bavaria, and the LMU*innovativ* Project Bioimaging Network (BIN) and by an Advanced Investigator grant from the European Research Council and an LMU*excellent* Research Professorship.

REFERENCES

1. **Abruzzi KC, Lacadie S, Rosbash M.** 2004. Biochemical analysis of TREX complex recruitment to intronless and intron-containing yeast genes. EMBO J. **23**:2620–2631.
2. **Ahn SH, Keogh M-C, Buratowski S.** 2009. Ctk1 promotes dissociation of basal transcription factors from elongating RNA polymerase II. EMBO J. **28**:205–212.
3. **Ahn SH, Kim M, Buratowski S.** 2004. Phosphorylation of serine 2 within the RNA polymerase II C-terminal domain couples transcription and 3′ end processing. Mol. Cell **13**:67–76.
4. **Amrani N, et al.** 1997. PCF11 encodes a third protein component of yeast cleavage and polyadenylation factor I. Mol. Cell. Biol. **17**:1102–1109.
5. **Andrulis ED, Guzmán E, Döring P, Werner J, Lis JT.** 2000. High-resolution localization of Drosophila Spt5 and Spt6 at heat shock genes in vivo: roles in promoter proximal pausing and transcription elongation. Genes Dev. **14**:2635–2649.
6. **Aranda A, Proudfoot N.** 2001. Transcriptional termination factors for RNA polymerase II in yeast. Mol. Cell **7**:1003–1011.
7. **Barillà D, Lee BA, Proudfoot NJ.** 2001. Cleavage/polyadenylation factor IA associates with the carboxyl-terminal domain of RNA polymerase II in Saccharomyces cerevisiae. Proc. Natl. Acad. Sci. U. S. A. **98**:445–450.
8. **Bentley DL.** 2005. Rules of engagement: co-transcriptional recruitment of pre-mRNA processing factors. Curr. Opin. Cell Biol. **17**:251–256.
9. **Birse CE, Minvielle-Sebastia L, Lee BA, Keller W, Proudfoot NJ.** 1998. Coupling termination of transcription to messenger RNA maturation in yeast. Science **280**:298–301.
10. **Buratowski S.** 2009. Progression through the RNA polymerase II CTD cycle. Mol. Cell **36**:541–546.
11. **Burmann BM, et al.** 2010. A NusE:NusG complex links transcription and translation. Science **328**:501–504.
12. **Chen H, et al.** 2009. Repression of RNA polymerase II elongation in vivo is critically dependent on the C-terminus of Spt5. PLoS One **4**:e6918.

13. **David L, et al.** 2006. A high-resolution map of transcription in the yeast genome. Proc. Natl. Acad. Sci. U. S. A. **103**:5320–5325.
14. **Dengl S, Mayer A, Sun M, Cramer P.** 2009. Structure and in vivo requirement of the yeast Spt6 SH2 domain. J. Mol. Biol. **389**:211–225.
15. **Dermody JL, Buratowski S.** 2010. Leo1 subunit of the yeast Paf1 complex binds RNA and contributes to complex recruitment. J. Biol. Chem. **285**: 33671–33679.
16. **Ding B, LeJeune D, Li S.** 2010. The C-terminal repeat domain of Spt5 plays an important role in suppression of Rad26-independent transcription coupled repair. J. Bio. Chem. **285**:5317–5326.
17. **Drouin S, Laramée L, Jacques P-É, Forest A, Bergeron M, Robert F.** 2010. DSIF and RNA polymerase II CTD phosphorylation coordinate the recruitment of Rpd3S to actively transcribed genes. PLoS Genet. **6**:e1001173.
18. **Egloff S, Murphy S.** 2008. Cracking the RNA polymerase II CTD code. Trends Genet. **24**:280–288.
19. **Fan X, Lamarre-Vincent N, Wang Q, Struhl K.** 2008. Extensive chromatin fragmentation improves enrichment of protein binding sites in chromatin immunoprecipitation experiments. Nucleic Acids Res. **36**: e125.
20. **Frohman MA, Dush MK, Martin GR.** 1988. Rapid production of full-length cDNAs from rare transcripts: amplification using a single gene-specific oligonucleotide primer. Proc. Natl. Acad. Sci. U. S. A. **85**:8998–9002.
21. **Gao L, Gross DS.** 2008. Sir2 silences gene transcription by targeting the transition between RNA polymerase II initiation and elongation. Mol. Cell. Biol. **28**:3979–3994.
22. **Glover-Cutter K, Kim S, Espinosa J, Bentley DL.** 2008. RNA polymerase II pauses and associates with pre-mRNA processing factors at both ends of genes. Nat. Struct. Mol. Biol. **15**:71–78.
23. **Gross S, Moore C.** 2001. Five subunits are required for reconstitution of the cleavage and polyadenylation activities of Saccharomyces cerevisiae cleavage factor I. Proc. Natl. Acad. Sci. U. S. A. **98**:6080–6085.
24. **Hartzog GA, Wada T, Handa H, Winston F.** 1998. Evidence that Spt4, Spt5, and Spt6 control transcription elongation by RNA polymerase II in Saccharomyces cerevisiae. Genes Dev. **12**:357–369.
25. **Hershkovits G, Bangio H, Cohen R, Katcoff DJ.** 2006. Recruitment of mRNA cleavage/polyadenylation machinery by the yeast chromatin protein Sin1p/Spt2p. Proc. Natl. Acad. Sci. U. S. A. **103**:9808–9813.
26. **Hirtreiter A, et al.** 2010. Spt4/5 stimulates transcription elongation through the RNA polymerase clamp coiled-coil motif. Nucleic Acids Res. **38**:4040–4051.
27. **Hocine S, Singer RH, Grünwald D.** 2010. RNA processing and export. Cold Spring Harb. Perspect. Biol. **2**:a000752.
28. **Jaehning, JA.** 2010. The Paf1 complex: platform or player in RNA polymerase II transcription? Biochim. Biophys. Acta **1799**:379–388.
29. **Johnson SA, Cubberley G, Bentley DL.** 2009. Cotranscriptional recruitment of the mRNA export factor Yra1 by direct interaction with the 3′ end processing factor Pcf11. Mol. Cell **33**:215–226.
30. **Kaplan CD, Holland MJ, Winston F.** 2005. Interaction between transcription elongation factors and mRNA 3′-end formation at the Saccharomyces cerevisiae GAL10-GAL7 locus. J. Biol. Chem. **280**:913–922.
31. **Kaplan CD, Morris JR, Wu C, Winston F.** 2000. Spt5 and Spt6 are associated with active transcription and have characteristics of general elongation factors in D. melanogaster. Genes Dev. **14**:2623–2634.
32. **Kessler MM, et al.** 1997. Hrp1, a sequence-specific RNA-binding protein that shuttles between the nucleus and the cytoplasm, is required for mRNA 3′-end formation in yeast. Genes Dev. **11**:2545–2556.
33. **Kessler MM, Zhao J, Moore CL.** 1996. Purification of the Saccharomyces cerevisiae cleavage/polyadenylation factor I. J. Biol. Chem. **271**:27167–27175.
34. **Kettenberger H, Armache K-J, Cramer P.** 2003. Architecture of the RNA polymerase II-TFIIS complex and implications for mRNA cleavage. Cell **114**:347–357.
35. **Kim M, Ahn S-H, Krogan NJ, Greenblatt JF, Buratowski S.** 2004. Transitions in RNA polymerase II elongation complexes at the 3′ ends of genes. EMBO J. **23**:354–364.
36. **Klein BJ, et al.** 2011. RNA polymerase and transcription elongation factor Spt4/5 complex structure. Proc. Natl. Acad. Sci. U. S. A. **108**:546–550.
37. **Knop M, et al.** 1999. Epitope tagging of yeast genes using a PCR-based strategy: more tags and improved practical routines. Yeast **15**:963–972.
38. **Knowlton JR, et al.** 2003. A spring-loaded state of NusG in its functional cycle is suggested by X-ray crystallography and supported by site-directed mutants. Biochemistry **42**:2275–2281.
39. **Komarnitsky P, Cho E-J, Buratowski S.** 2000. Different phosphorylated forms of RNA polymerase II and associated mRNA processing factors during transcription. Genes Dev. **14**:2452–2460.
40. **Larson DR, Zenklusen D, Wu B, Chao JA, Singer RH.** 2011. Real-time observation of transcription initiation and elongation on an endogenous yeast gene. Science **332**:475–478.
41. **Leeper TC, Qu X, Lu C, Moore C, Varani G.** 2010. Novel protein-protein contacts facilitate mRNA 3′-processing signal recognition by Rna15 and Hrp1. J. Mol. Biol. **401**:334–349.
42. **Li B, Carey M, Workman JL.** 2007. The role of chromatin during transcription. Cell **128**:707–719.
43. **Licatalosi DD, et al.** 2002. Functional interaction of yeast pre-mRNA 3′ end processing factors with RNA polymerase II. Mol. Cell **9**:1101–1111.
44. **Lindstrom DL, et al.** 2003. Dual roles for Spt5 in pre-mRNA processing and transcription elongation revealed by identification of Spt5-associated proteins. Mol. Cell. Biol. **23**:1368–1378.
45. **Liu Y, et al.** 2009. Phosphorylation of the transcription elongation factor Spt5 by yeast Bur1 kinase stimulates recruitment of the PAF complex. Mol. Cell. Biol. **29**:4852–4863.
46. **Luna R, Gaillard H, González-Aguilera C, Aguilera A.** 2008. Biogenesis of mRNPs: integrating different processes in the eukaryotic nucleus. Chromosoma **117**:319–331.
47. **Lunde BM, et al.** 2010. Cooperative interaction of transcription termination factors with the RNA polymerase II C-terminal domain. Nat. Struct. Mol. Biol. **17**:1195–1201.
48. **Mandart E, Parker R.** 1995. Effects of mutations in the Saccharomyces cerevisiae RNA14, RNA15, and PAP1 genes on polyadenylation in vivo. Mol. Cell. Biol. **15**:6979–6986.
49. **Mandel C, Bai Y, Tong L.** 2008. Protein factors in pre-mRNA 3′-end processing. Cell. Mol. Life Sci. **65**:1099–1122.
50. **Martin W, Koonin EV.** 2006. Introns and the origin of nucleus-cytosol compartmentalization. Nature **440**:41–45.
51. **Martinez-Rucobo FW, Sainsbury S, Cheung ACM, Cramer P.** 2011. Architecture of the RNA polymerase-Spt4/5 complex and basis of universal transcription processivity. EMBO J. **30**:1302–1310.
52. **Mayer A, et al.** 2010. Uniform transitions of the general RNA polymerase II transcription complex. Nat. Struct. Mol. Biol. **17**:1272–1278.
53. **Meinhart A, Cramer P.** 2004. Recognition of RNA polymerase II carboxy-terminal domain by 3′-RNA-processing factors. Nature **430**:223–226.
54. **Meinhart A, Kamenski T, Hoeppner S, Baumli S, Cramer P.** 2005. A structural perspective of CTD function. Genes Dev. **19**:1401–1415.
55. **Millevoi S, Vagner S.** 2010. Molecular mechanisms of eukaryotic pre-mRNA 3′ end processing regulation. Nucleic Acids Res. **38**:2757–2774.
56. **Minvielle-Sebastia L, et al.** 1998. Control of cleavage site selection during mRNA 3′ end formation by a yeast hnRNP. EMBO J. **17**:7454–7468.
57. **Minvielle-Sebastia L, Preker P, Keller W.** 1994. RNA14 and RNA15 proteins as components of a yeast pre-mRNA 3′-end processing factor. Science **266**:1702–1705.
58. **Minvielle-Sebastia L, Preker PJ, Wiederkehr T, Strahm Y, Keller W.** 1997. The major yeast poly(A)-binding protein is associated with cleavage factor IA and functions in premessenger RNA 3′-end formation. Proc. Natl. Acad. Sci. U. S. A. **94**:7897–7902.
59. **Mooney RA, Schweimer K, Rösch P, Gottesman M, Landick R.** 2009. Two structurally independent domains of E. coli NusG create regulatory plasticity via distinct interactions with RNA polymerase and regulators. J. Mol. Biol. **391**:341–358.
60. **Mueller CL, Porter SE, Hoffman MG, Jaehning JA.** 2004. The Paf1 complex has functions independent of actively transcribing RNA polymerase II. Mol. Cell **14**:447–456.
61. **Nagalakshmi U, et al.** 2008. The transcriptional landscape of the yeast genome defined by RNA sequencing. Science **320**:1344–1349.
62. **Nordick K, Hoffman MG, Betz JL, Jaehning JA.** 2008. Direct interactions between the Paf1 complex and a cleavage and polyadenylation factor are revealed by dissociation of Paf1 from RNA polymerase II. Eukaryot. Cell **7**:1158–1167.
63. **Pancevac C, Goldstone DC, Ramos A, Taylor IA.** 2010. Structure of the Rna15 RRM-RNA complex reveals the molecular basis of GU specificity in transcriptional 3′-end processing factors. Nucleic Acids Res. **38**:3119–3132.
64. **Pavri R, et al.** 2010. Activation-induced cytidine deaminase targets DNA

at sites of RNA polymerase II stalling by interaction with Spt5. Cell **143**: 122–133.
65. **Pei Y, Shuman S.** 2002. Interactions between fission yeast mRNA capping enzymes and elongation factor Spt5. J. Biol. Chem. **277**:19639–19648.
66. **Perales R, Bentley D.** 2009. "Cotranscriptionality": the transcription elongation complex as a nexus for nuclear transactions. Mol. Cell **36**:178–191.
67. **Pérez-Cañadillas JM.** 2006. Grabbing the message: structural basis of mRNA 3′ UTR recognition by Hrp1. EMBO J. **25**:3167–3178.
68. **Pokholok DK, Hannett NM, Young RA.** 2002. Exchange of RNA polymerase II initiation and elongation factors during gene expression in vivo. Mol. Cell **9**:799–809.
69. **Ponting CP.** 2002. Novel domains and orthologues of eukaryotic transcription elongation factors. Nucleic Acids Res. **30**:3643–3652.
70. **Proshkin S, Rahmouni AR, Mironov A, Nudler E.** 2010. Cooperation between translating ribosomes and RNA polymerase in transcription elongation. Science **328**:504–508.
71. **Proudfoot N.** 2004. New perspectives on connecting messenger RNA 3′ end formation to transcription. Curr. Opin. Cell Biol. **16**:272–278.
72. **Qu X, et al.** 2009. Assembly of an export-competent mRNP is needed for efficient release of the 3′-end processing complex after polyadenylation. Mol. Cell. Biol. **29**:5327–5338.
73. **Sadowski M, Dichtl B, Hubner W, Keller W.** 2003. Independent functions of yeast Pcf11p in pre-mRNA 3′ end processing and in transcription termination. EMBO J. **22**:2167–2177.
74. **Schneider DA, et al.** 2006. RNA polymerase II elongation factors Spt4p and Spt5p play roles in transcription elongation by RNA polymerase I and rRNA processing. Proc. Natl. Acad. Sci. U. S. A. **103**:12707–12712.
75. **Schneider S, Pei Y, Shuman S, Schwer B.** 2010. Separable functions of the fission yeast Spt5 carboxyl-terminal domain (CTD) in capping enzyme binding and transcription elongation overlap with those of the RNA polymerase II CTD. Mol. Cell. Biol. **30**:2353–2364.
76. **Shen Z, St-Denis A, Chartrand P.** 2010. Cotranscriptional recruitment of She2p by RNA pol II elongation factor Spt4-Spt5/DSIF promotes mRNA localization to the yeast bud. Genes Dev. **24**:1914–1926.
77. **Swanson MS, Malone EA, Winston F.** 1991. SPT5, an essential gene important for normal transcription in Saccharomyces cerevisiae, encodes an acidic nuclear protein with a carboxy-terminal repeat. Mol. Cell. Biol. **11**:3009–3019.
78. **Swanson MS, Winston F.** 1992. SPT4, SPT5 and SPT6 interactions: effects on transcription and viability in Saccharomyces cerevisiae. Genetics **132**:325–336.
79. **Swinburne IA, Meyer CA, Liu XS, Silver PA, Brodsky AS.** 2006. Genomic localization of RNA binding proteins reveals links between pre-mRNA processing and transcription. Genome Res. **16**:912–921.
80. **Venters BJ, Pugh BF.** 2009. How eukaryotic genes are transcribed. Crit. Rev. Biochem. Mol. Biol. **44**:117–141.
81. **Venters BJ, et al.** 2011. A comprehensive genomic binding map of gene and chromatin regulatory proteins in Saccharomyces. Mol. Cell **41**:480–492.
82. **Viktorovskaya OV, Appling FD, Schneider DA.** 2011. Yeast transcription elongation factor SPT5 associates with RNA polymerase I and RNA polymerase II directly. J. Biol. Chem. **286**:18825–18833.
83. **Wada T, et al.** 1998. DSIF, a novel transcription elongation factor that regulates RNA polymerase II processivity, is composed of human Spt4 and Spt5 homologs. Genes Dev. **12**:343–356.
84. **Wen Y, Shatkin AJ.** 1999. Transcription elongation factor hSPT5 stimulates mRNA capping. Genes Dev. **13**:1774–1779.
85. **Werner F, Grohmann D.** 2011. Evolution of multisubunit RNA polymerases in the three domains of life. Nat. Rev. Microbiol. **9**:85–98.
86. **Winston F, Chaleff DT, Valent B, Fink GR.** 1984. Mutations affecting Ty-mediated expression of the HIS4 gene of Saccharomyces cerevisiae. Genetics **107**:179–197.
87. **Yamada T, et al.** 2006. P-TEFb-mediated phosphorylation of hSpt5 C-terminal repeats is critical for processive transcription elongation. Mol. Cell **21**:227–237.
88. **Zhang Z, Fu J, Gilmour DS.** 2005. CTD-dependent dismantling of the RNA polymerase II elongation complex by the pre-mRNA 3′-end processing factor, Pcf11. Genes Dev. **19**:1572–1580.
89. **Zhou K, Kuo WHW, Fillingham J, Greenblatt JF.** 2009. Control of transcriptional elongation and cotranscriptional histone modification by the yeast BUR kinase substrate Spt5. Proc. Natl. Acad. Sci. U. S. A. **106**: 6956–6961.